Ultrathin Films of Organic Networks as Nanofiltration Membranes via Solution-Based Molecular Layer Deposition

ARTICLE *in* LANGMUIR · DECEMBER 2012

Impact Factor: 4.46 · DOI: 10.1021/la304196q · Source: PubMed

4 AUTHORS, INCLUDING:

Shenghai Li
Chinese Academy of Sciences
48 PUBLICATIONS **1,950** CITATIONS
SEE PROFILE

Jifu Zheng
Chinese Academy of Sciences
20 PUBLICATIONS **160** CITATIONS
SEE PROFILE

Langmuir

Article

pubs.acs.org/Langmuir

Ultrathin Films of Organic Networks as Nanofiltration Membranes via Solution-Based Molecular Layer Deposition

Huidong Qian,[†,‡] Shenghai Li,[†] Jifu Zheng,[†] and Suobo Zhang*[,†]

[†]Key Laboratory of Polymer Ecomaterials, Changchun Institute of Applied Chemistry, Chinese Academy of Sciences, Changchun 130022, China

[‡]Graduate School of the Chinese Academy of Sciences, Beijing 100039, China

Supporting Information

ABSTRACT: Ultrathin films of organic networks on various substrates were fabricated through the solution-based molecular layer deposition (MLD) technique. The rigid tetrahedral geometries of polyfunctional amine and acyl chloride involved in the reaction ensure the continuity of the polymerization process. A linear increase in film thickness with respect to cycle number was observed by UV−vis adsorption, ellipsometry, and quartz crystal microbalance. The growth rate per MLD cycle is 1.6 nm, which can be controlled at the single molecular level. For the first time, we develop the MLD method on the top of hydrolyzed PAN substrate, resulting in nanofiltration (NF) membranes. The stepwise growth was monitored via attenuated total reflectance infrared studies. The separation performance of the obtained membrane for various solutes was sensitive to the terminated layers and number of cycles. The rejection of NH_2-terminated membranes follows the order of $CaCl_2$ > Na_2SO_4 > NaCl, while the order for COOH-capped surface is Na_2SO_4 > $CaCl_2$ > NaCl. The absolute value of zeta potential for the MLD membranes decreases with the addition of deposition layers. The moderate water flux for the resulting membrane is due to the reduced porosity of the support as well as the low roughness and hydrophilicity of the membrane surface. This bottom-up process provides a promising approach for construction of long-term steady NF membranes with nanoscale dimensions.

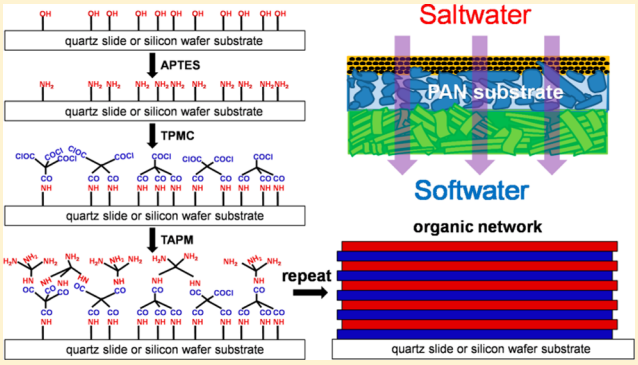

INTRODUCTION

The investigation and development of energy-efficient organic network materials have become a significant research topic in dealing with global issues such as carbon capture and storage (CCS) and water purification.[1] Saving resources, being friendly to the environment and with a clean production process, the membrane technology has been widely used in industry manufacture. However, most of these organic network materials are insoluble powders as the processability of organic networks into membranes or films is often difficult. Molecular layer deposition (MLD) is a layer-by-layer (LbL) thin film deposition method through the sequential self-limiting surface reaction at the single molecular level and has attracted increasing attention due to its readily fabrication of highly conformal multilayers with covalent linkages.[2] Compared with LbL assembly methods on the basis of noncovalent interactions, i.e., Coloumbic interations[3] and hydrogen bonding,[4,5] covalently bonded LbL films possess higher chemical stability due to the chemical nature of cross-linked polymer networks.[6−10] Although MLD technique was demonstrated earlier in 1991,[11] very few developments have occurred over the past decade. To date, most MLD processes are based on bifunctional monomers under vacuum conditions and have been reported for the growth of organic polymers such as polyamides,[12,13] polyimides,[14] polyurethanes,[15] and polyureas.[16−18] These systems are limited in a number of ways: (i) the large organic precursors generally have low vapor pressure, and they will decompose at high temperature;[12] (ii) it is hard to employ catalysts or to utilize solvent effects in vacuum-based reaction;[16] (iii) the "double reactions" between two ends of the bifunctional reactants will prevent the growth of polymer chains, resulting in growth rates that are less than the ideal bilayer unit length.[17] The solution-based MLD with multifunctional monomers may offer a way to overcome some of these problems.[19] In pioneering work by Park et al., a pair of tetrakis(4-aminophenyl)methane (TAPM) and tetrakis(4-isocyanatophenyl)methane (TIPM) was employed via solution-based MLD to prepare thin film organic molecular networks.[19] The principle is when these tetrahedral molecules react with the functional groups of the surfaces, at least one of the four vertices should remain intact and constitute the top surface of the growing film, leading to alternating deposition of TIPM and TAPM onto the substrate surface. Unfortunately, the ultrathin films were merely deposited on quartz slide or

Received: October 23, 2012
Revised: November 30, 2012
Published: December 2, 2012

silicon wafer substrates; other porous substrates have not been explored yet. Other cross-linked polyamide networks based on trimesoyl chloride (TMC) and *m*-phenylenediamine (MPD) by the MLD technique were also reported for the preparation of thin films,[20,21] but the substrates were quartz or Si wafer all the same.

Herein, we demonstrate the preparation and characterization of organic networks based on a pair of rigid tetraphenylmethane-4,4′,4″,4‴-tetraacyl chloride (TPMC) and TAPM via solution-based MLD method on quartz slide, silicon wafer, and Ag-coated quartz electrodes. The specific chemical system of forming covalent interlayer linkages is based on the reaction of acid chlorides with amines to produce amide groups. The choice of the two monomers is based on their ability to regenerate NH_2 and COCl functional groups on the surface at each growth step. Furthermore, this method was applied on porous polyacrylonitrile (PAN) substrates, resulting in nanofiltration (NF) membranes. The film thickness and charge of the outer surface of the membranes can be controlled easily by varying the number of deposition cycles. To the best of our knowledge, this is the first example of thin film of organic network on a porous substrate via MLD. In addition, the application of composite membranes in separation mono- and multivalent salts is investigated in detail.

EXPERIMENTAL SECTION

Materials. Tetrakis(4-aminophenyl)methane (TAPM) and tetraphenylmethane-4,4′,4″,4‴-tetraacyl chloride (TPMC) were synthesized according to the previously reported procedure[22] with some modifications. (3-Aminopropyl)triethoxysilane (APTES, >99%) was purchased from Alfa Aesar and used as received. High-purity carbon monoxide (99.99%) was obtained from Dalian Airchem Specialty Gases & Chemicals Co., Ltd. High-purity hydrogen (99.999%) was obtained from Changchun Juyang Gas, Co., Ltd. Tetrahydrofuran (THF) and toluene were distilled from sodium/potassium alloy with benzophenone in a nitrogen atmosphere. *N*,*N*-Dimethylformamide (DMF) and *N*-methylpyrrolidinone (NMP) were dried over CaH_2, distilled under reduced pressure and stored over 4 Å molecular sieves. All other solvents and reagents were in chemically pure grade and used as purchased unless otherwise noted.

Fabrication of Multilayer Films on Hard Substrates. Quartz slides (10 × 40 mm^2) and silicon (100) wafers (15 × 15 mm^2) were cleaned by sonication in pentane, acetone, and Milli-Q quality water (18.2 MΩ cm at 25 °C). Then the surfaces were treated with hot piranha solution (H_2SO_4 (98%)−H_2O_2 (30%) 70:30, v/v) for 40 min, rinsed thoroughly with Milli-Q water, and dried with N_2. (**Caution!** *Piranha solution is a very strong oxidant and should be handled with extreme care.*) After cleaning, the oxidized substrates were immersed in anhydrous toluene solution (50 mL) containing APTES (1 mL) for 24 h in a desiccator under an Ar atmosphere. After taking out of the solution, they were rinsed with anhydrous toluene and MeOH and dried with a N_2 stream. The APTES-modified substrates were then heated to 100 °C for 3 h under reduced pressure. The first cycle of deposition (referred to as 1 bilayer) was fabricated using the following procedure: (i) NH_2-functionalized substrates were placed into a solution of TPMC and Et_3N in THF (2 and 0.2 mM for TPMC and Et_3N, respectively) for 20 s, followed by rinsing with THF, toluene, and THF; (ii) (acid chloride)-terminated surfaces were submerged in a solution of TAPM in THF (2 mM) for 20 s, followed by rinsing with THF, DMF, and THF. The described procedure was repeated multiple times to fabricate multilayer films that can be used for characterization.

Fabrication of Multilayer Films on Porous Polyacrylonitrile Substrate. Polyacrylonitrile (PAN, Ande Membrane Separation Technology & Engineering, Co., Ltd., Beijing, China) with molecular weight cutoffs of 10 kDa was first hydrolyzed by immersing it completely into a 2 M NaOH solution at 40 °C for 2 h and then a 2 M HCl solution at room temperature for 0.5 h.[23] The hydrolyzed PAN substrates (PAN-COOH) were then washed with an excess amount of Milli-Q water and carefully cut into a suitable circular size to be used in the membrane testing cell. For the deposition of multilayers, PAN-COOH were first dried in a vacuum oven at 40 °C for at least 12 h to remove moisture and submerged in a solution of TAPM in THF (2 mM) for 20 s, followed by rinsing with THF, DMF, and THF (ii), then placed into a solution of TPMC and Et_3N in THF (2 and 0.2 mM for TPMC and Et_3N, respectively) for 20 s, followed by rinsing with THF, toluene, and THF (i). The described procedure was repeated multiple times to fabricate composite membranes that can be used for separation. To terminate the reaction, soak the wafer in water for 10 min, wash with ethanol, and dry with N_2. After deposition of the desired number of cycles, membranes were stored in water until use.

Bulk Synthesis of Polyamide Networks (BPA). BPA was prepared according to the literature procedure.[24] A mixture of TPMC (1.141 g, 2 mmol) and TAPM (0.761 g, 2 mmol) was dissolved in 10 mL of dry NMP under an Ar atmosphere. Then the mixture was stirred at room temperature for 0.5 h, 80 °C for 1 h, and 150 °C for 4 h. After cooling, the reaction mixture was poured into MeOH (100 mL), and the purplish-red precipitate was filtered off, washed with DMF and MeOH, and dried in vacuo (100 °C, 12 h) to afford BPA (1.465 g, 91%).

Characterization. ^1H and ^{13}C NMR spectra were measured on the Bruker Avance 300 or 600 MHz spectrometer. UV−vis spectra of the thin films deposited on quartz slides were collected on a Shimadzu UV-1800 spectrophotometer. A bare quartz slide coated with an APTES monolayer was used as a reference. The thickness of the organic networks deposited on the silicon substrate after a set number of cycles (5, 10, 20, and 30) was monitored by a variable angle spectroscopic ellipsometer (Model VASE, J.A. Woollam Inc., Lincoln, NE), using a 70° angle of incidence. The thickness was calculated by Cauchy's equation assuming the films to be homogeneous and smooth and a constant film refractive index of $n = 1.5$.[20] All reported ellipsometric thicknesses represent an average over five different spots on the same wafer. The thickness of APTES monolayer was used as a baseline thickness, which was subtracted from the subsequent total film thickness to yield the thickness of deposited organic layer. Attenuated total reflectance infrared (ATR-IR) characterization of the MLD membranes on PAN-COOH substrate was performed by a Bio-Rad Digilab Division FST-80 spectrometer. For ATR-IR analysis of membrane samples, Irtran crystal at 45° angle of incidence was employed. The FT-IR spectra were obtained using a Bruker Vertex 70 spectrometer at a nominal resolution of 2 cm^{-1}. Static contact angles of water for the MLD membranes on PAN-COOH substrate were measured by the sessile drop method with a 2 μL water droplet using a Drop Shape Analysis DSA10 (Krüss Gmbh, Germany) at ambient temperature. At least eight measurements were taken for each sample. The atomic force microscopy (AFM) images of the multilayered films on PAN-COOH were performed on the SPA300HV with an SPI 3800 controller (Seiko Instruments Industry Co. Ltd.). All the tapping mode images were taken at ambient temperature in air with the rectangle crystal Si cantilevers (Budget Sensors). The topography images were obtained at a resonance frequency of ∼320 kHz for the probe oscillation. A homemade quartz crystal microbalance (QCM) was used to detect the mass of the deposited layers using a 9 MHz quartz electrode coated with Ag on both sides. Prior to measurements, QCM sensors were exposed to a N_2 stream until a stable baseline was reached. The QCM frequency shifts were monitored with a Protek C3100 universal frequency counter, and the mass of deposited layer was calculated from the Sauerbrey equation[25]

$$\Delta m = -\frac{\rho_q l_q}{f_0}\frac{\Delta f}{n}$$

where f_0 is the fundamental frequency, ρ_q and l_q are the density and thickness of the quartz crystal, n is the overtone number, Δm is the change in mass, and Δf is the observed residual frequency shift. The Sauerbrey equation can be shortly written as $\Delta m = -C\Delta f$, where C is mass sensitivity, which is 2.73 ng/cm^2 in our system.

dx.doi.org/10.1021/la304196q | *Langmuir* 2012, 28, 17803−17810

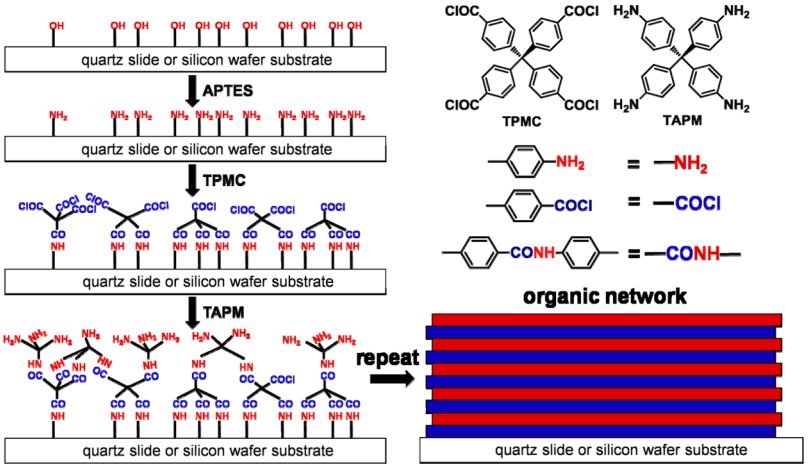

Figure 1. Schematic illustration of molecular layer deposition process on planar substrates and chemical structures of TPMC and TAPM.

The nanofiltration (NF) performance tests were conducted using a cross-flow filtration system at 0.4 MPa with an effective membrane area of 20.4 cm^2. Compaction was performed at an applied pressure of 0.5 MPa for 4 h prior to the measurement. The salt rejection rate was measured by the salt concentration in the permeation and the feed using an Elmeiron conductivity meter CC-501 (Poland). The desalination rate was calculated by using the equation

$$R_j\ (\%) = \left(1 - \frac{c_p}{c_f}\right) \times 100$$

where c_p (mg/L) is the permeate concentration and c_f (mg/L) is the feed concentration (500 mg/L). All membrane samples were prepared and tested in at least duplicated with a total of three membranes tests for NF performance, the results of which have been averaged.

Surface streaming potential of the membranes was performed with a homemade streaming potential analyzer according to Yu et al.[26] A 10 mM KCl solution adjusted to pH 6.5 with HCl and KOH solutions was used as the electrolyte. Measurements were carried out at five pressure differences ranging from 0.1 to 0.5 MPa. The zeta potential was calculated from the Helmholtz–Smoluchowski equation with the Fairbrother and Mastin substitution[27]

$$\zeta = \frac{\Delta E}{\Delta P} \frac{\eta\kappa}{\varepsilon\varepsilon_0}$$

where ζ is the zeta potential, ΔE is the electrical potential difference, ΔP is the applied pressure, η is the viscosity of the solution, κ is the solution conductivity, and ε and ε_0 are the permittivity of the test solution and free space, respectively.

RESULTS AND DISCUSSION

Multilayer Growth. Different substrates, such as quartz slides, silicon wafers, and Ag-coated quartz electrodes, were used in this work, which were determined by the measurements to be performed. In order to create a monolayer system of the deposition, we employed TPMC/TAPM pair as structural motifs because the rigid tetrahedral geometries of TPMC and TAPM ensure the continuity of the polymerization process. The general procedure for fabrication of polyamide networks via MLD is depicted in Figure 1, which is similar to the case of polyurea networks.[19] The modification of the initial surface prior to the deposition was first carried out by exposing oxidized quartz slide or Si wafer substrates to APTES. Then the amine-terminated substrates were sequentially immersed in a freshly solution of TPMC and a solution of TAPM in the presence of Et_3N as a base, and each immersion step was followed by a rinsing step. The high reactivity of acid chlorides to amines is deemed to occur on the order of 1 s;[21,28] an extra time of 20 s was enough for the complete conversion.

The growth behavior of bilayers rather than monolayers on quartz slides, silicon wafers, and Ag-coated quartz electrodes was tested due to the sensitivity of terminal acid chloride groups to hydrolyze to carboxylic acids. Figure 2 shows the

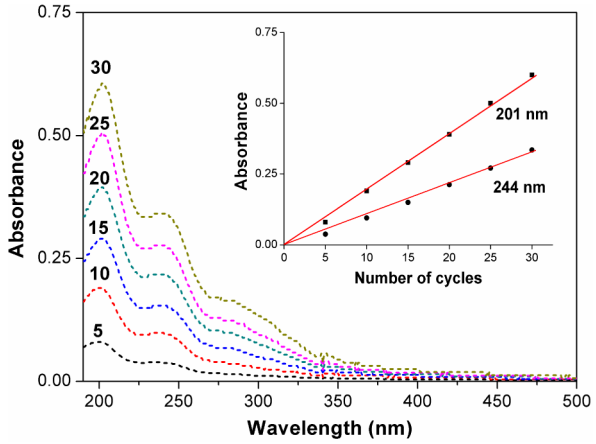

Figure 2. UV–vis spectra of multilayer films as a function of deposition cycle number on quartz slides. Inset: absorption peaks intensities at 201 and 244 nm as a function of deposition cycle number.

UV–vis absorption spectra of multilayer films via MLD with an increasing number of deposition cycles. The two absorption peaks centered at 201 and 244 nm correspond to π–π^* transition of phenyl rings in the polyamide network.[25] The inset displays the UV absorbance at these two wavelengths against the number of deposition cycle, and a linear growth pattern is clearly observed. The uniform film formation indicates the self-limiting feature of MLD. The chemical stability of covalently bonded TPMC/TAPM networks (30 cycles) was tested in both acidic and basic conditions.[29] All the films are quite stable without significant change in UV–vis spectra after they were immersed in pH 1 and 10 solutions at room temperature for 12 h (Figure S7).

Thicknesses of MLD Films. The thicknesses of different cycled organic networks were obtained by ellipsometry and quartz crystal microbalance (QCM) for verification. As shown in Figure 3, the film thickness subtracted from the first APTES

dx.doi.org/10.1021/la304196q | Langmuir 2012, 28, 17803–17810

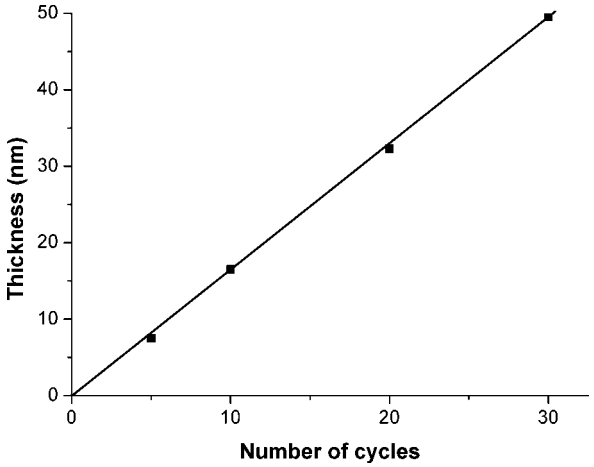

Figure 3. Film thickness as a function of deposition cycle number.

monolayer (~6.4 Å) increases linearly with increasing cycle number, in accordance with the UV−vis data. The average growth rate is 1.64 nm per TPMC/TAPM cycle, which is in close agreement with the molecular modeling (Figure S8). We optimized the molecular geometries of TPMC and TAPM using the density functional theory (DFT) with Becke's three-parameter hybrid method combining with the Lee−Yang−Parr correlation functional (B3LYP).[30,31] The 6-31G* basis set was employed, and all calculations were performed with the B.01 revision of the Gaussian 09 program package.[32] For TPMC, the distance between every two vertices (acyl carbon atoms) in the corresponding regular tetrahedron (a) is 9.20 Å and the height from one apex to the opposite faces (h) is 7.51 Å. Thus, the growth rate of a TPMC layer must be in the range 7.51−9.20 Å. As for TAPM, the growth rate is in the range 7.41−9.07 Å, and thus the combined molecular length of per TPMC/TAPM cycle is calculated approximately to be in the range 14.92−18.27 Å.

The mass increase during the deposition process was investigated by the QCM frequency shifts. As can be seen in Figure 4, the QCM frequency decreases regularly with the increasing number of cycles, resulting in an overall constant frequency decrease rate of 70 ± 2 Hz per TPMC/TAPM cycle. By applying the Sauerbrey equation, these frequency shifts correspond to a mass increase of 191.1 ng/cm^2 for a deposition

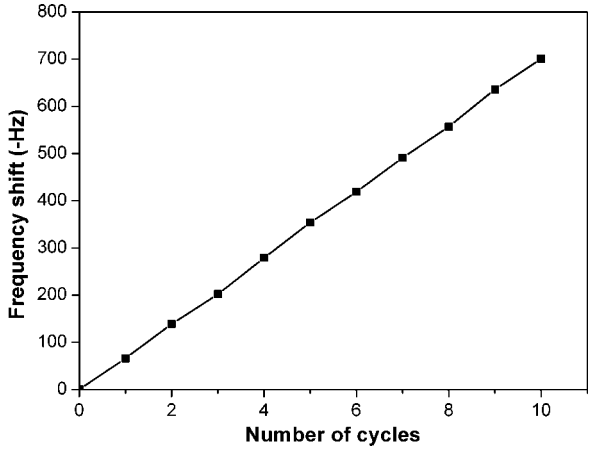

Figure 4. QCM frequency shifts vs number of MLD cycle for alternating depositions of TPMC and TAPM.

cycle. Assuming the density of the multilayer films is 1.0 g/cm^3, the thickness of per cycle is estimated to be 1.91 nm, which is beyond the scope of 14.92−18.27 Å. It results from the underestimation of the polyamide density. However, it is difficult to determine the film density as the adsorbed ultrathin films cannot be peeled off from the substrates. Thus, we synthesized the bulk polyamide networks (BPA) by reacting equimolar amounts of TPMC and TAPM in dry NMP under an Ar atmosphere, whose structure can be confirmed by FT-IR (Figure S9). The density of BPA, determined by measurements of the weight in air and in the EtOH at 25.0 °C using Archimedes' principle, was 1.21 g cm^{-3}, which was similar to the reported poly(*p*-phenylene terephthalamide) (PPTA) of 1.26 g cm^{-3}.[13] Consequently, the TPMC/TAPM MLD growth rate from QCM is estimated to be 1.58 nm per cycle, in accordance with the ellipsometry results.

MLD NF Membranes. The successful fabrication of organic networks on these substrates encouraged us to develop the MLD method on porous PAN substrate which can be used as NF membranes. NF is a pressure-driven membrane separation process normally applicable for separating divalent ions or dissolved components having a molecular weight range from 200 to 1000.[33] Multilayered polyelectrolytes based on polycations and polyanions as actual separation layers of composite membranes for NF have been well studied;[34] however, the MLD technique has not been employed for NF membranes yet. For our studies, in order to promote stable ionic bonding between the first molecular layer and the support, we initially hydrolyzed PAN substrates according to reported procedure[23] and denoted them as PAN-COOH. Then PAN-COOH was sequentially immersed in TAPM and TPMC in the presence of Et_3N as a base, which was opposite to the order of deposition on hard substrates. Multilayered films can be formed as skin layers when the procedure was repeated. The expression of $(TAPM/TPMC)_n$TAPM means TAPM is the top layer in the deposited films and *n* is the number of deposited cycles, while $(TAPM/TPMC)_n$ indicates the membranes terminate with a TPMC layer, resulting in a carboxylic acid-terminated surface when the acid chloride groups were hydrolyzed.

ATR-IR spectra confirm the deposition of $(TAPM/TPMC)_n$ networks on PAN-COOH supports (Figure 5). The ATR-IR

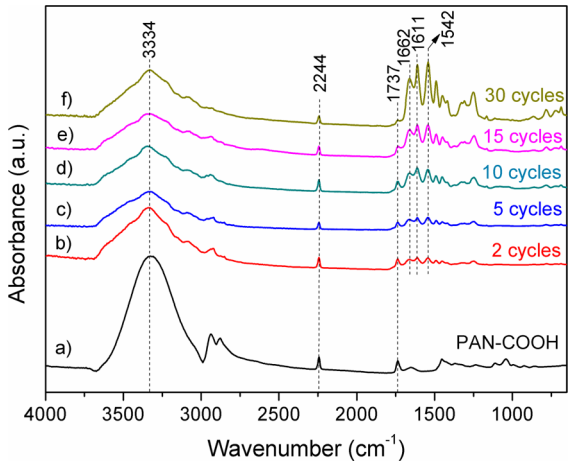

Figure 5. ATR-IR spectra of (a) PAN-COOH substrate and after various number of deposition cycles: (b) 2, (c) 5, (d) 10, (e) 15, and (f) 30 cycles.

dx.doi.org/10.1021/la304196q | *Langmuir* 2012, 28, 17803−17810

technique reveals chemical structure information for 0.1−1 μm depth of the surface; thus, the absorbance spectrum is a combination of skin layer and PAN-COOH matrix. Compared with the absorbance spectra of pristine PAN (Figure S10), the intensity of −CN stretching peak at 2244 cm^{-1} decreases after parial hydrolysis of −CN groups into −COOH groups (Figure 5a). The peak at 1737 cm^{-1} maybe associated with the presence of the comonomer viny acetate or minor structural defects formed during polymer synthesis or degradation.[35] Other assignments of observed absorbance peaks of PAN-COOH substrate are indicated as shown in Figure S10. Although large background absorbance of COOH from the support obscures the generated terminal COOH groups, it is evident from Figure 5a−f that with the deposition of TAPM/TPMC layers onto the PAN-COOH substrate new peaks occurred at 1662 and 1542 cm^{-1}, which can be assigned to the characteristic vibration C═O stretching (amide I) and (C═O)N−H bending and C−N stretching (amide II), respectively. In addition, the characteristic peak of the aromatic ring breathing is observed at 1611 cm^{-1}. The absence of any −COCl mode near 1777 cm^{-1} suggests the acid chloride has completely reacted with the amine to produce covalent amide linkages. These absorbance features are all consistent with the FT-IR spectrum of the bulk polyamide (Figure S9), confirming the incorporation of amide interlayer linkages into the polymer networks. Furthermore, the relative peak area of amide II increases gradually with increasing number of MLD cycles, indicating the characteristic modes of the MLD networks (Table S1).

NF Performance. A key objective of our studies was to test NF performance of MLD membranes. The salt filtration characteristics of the membranes were studied in terms of three different solutes: NaCl, $CaCl_2$, and Na_2SO_4 with a feed concentration of 500 mg/L, and the experimental results are presented in Table 1. For all solutions, water flux decreases monotonically with an increasing number of deposited cycles because of increasing film thickness. TAPM/TPMC membranes also show an impressive divalent ion rejection that varies with the charge of the outermost layer of the membrane. The NH_2-terminated membranes will be positively charged due to the protonation of the NH_2 groups, while the COOH-terminated membrane is negatively charged. For example, $CaCl_2$ rejection of $(TAPM/TPMC)_{15}$ increases from 70.9% to 93.3% after deposition of a terminal TPMC layer. Correspondingly, Na_2SO_4 rejection decreases from 93.5% to 74.8%. The opposite trend is observed for Na_2SO_4, while NaCl rejection has little dependence on the terminal layers (the salt rejection increases continuously as the deposition cycle increases) because the anion and cation in the NaCl have the same magnitude of charge.[36] We would also expect the salt rejection of $(TAPM/TPMC)_{15}TAPM$ follows the order of $CaCl_2$ > NaCl > Na_2SO_4 because Ca^{2+} is more easily rejected than Na^+ as it is more easily repelled from the positively charged surfaces and Cl^- is more easily repelled due to the strong affinity between SO_4^{2-} and NH_2 groups on the membrane surface.[37] However, the fact is the salt rejection follows the order of $CaCl_2$ > Na_2SO_4 > NaCl, which may be result from the bigger size of SO_4^{2-} than Cl^- (the Born radius for SO_4^{2-} and Cl^- is 0.258 and 0.202 nm, respectively, and Born radius is defined to exactly yield the measured energy of hydration in water[38]). This suggests the salt rejection for MLD membrane is not only related with the electrostatic repulsion (Donnan effect) but also depends on the size exclusion effect.

Table 1. Water Flux, Salts Rejection, Zeta Potential, and Contact Angle (CA) for Various MLD NF Membranes

no. of cycles[a]	water flux[b] (L/(m² h))	rejection (%)[b] NaCl	$CaCl_2$	Na_2SO_4	zeta potential[c] (mV)	CA (deg)
0	246.7	9.5	0.6	26.7	−32.4	28.4
2	190.4	11.0	36.3	63.4	−33.5	34.2
2.5	181.2	11.7	56.9	32.6	29.0	36.5
5	125.6	17.4	41.5	75.4	−30.7	45.6
5.5	118.3	19.8	77.3	49.8	28.6	47.3
10	71.1	26.6	60.0	87.4	−28.4	58.5
10.5	65.2	27.1	87.7	59.6	25.8	60.9
14.5	45.6	33.2	91.6	71.4	24.9	66.7
15	43.8	34.3	70.9	93.5	−26.1	65.6
15.5	35.7	35.1	93.3	74.8	24.3	69.1
30	11.2	46.0	83.3	97.2	−19.7	77.5
30.5	9.5	47.3	97.4	82.1	17.6	79.6

[a]Integer numbers of cycles indicate films terminated with TPMC, while films with an extra 0.5 cycles are terminated with TAPM. [b]The salt solutions were 500 mg/L, and NF was performed at 0.4 MPa. [c]Data deduced from streaming potential measurements at pH 6.0 in 10 mM KCl electrolyte.

The streaming potential is widely used in the studying of surface property of the membrane.[39] Thus, we investigated the zeta potential of membrane surfaces at a pH of 6.0 using 10 mM KCl electrolyte. As listed in Table 1, the zeta potential alternates after each new TAPM or TPMC deposition, becoming successively positive or negative. The PAN-COOH substrate has a negative zeta potential of −32.4 mV, which is similar to the reported data of −30 ± 1.0 mV,[35] and the value shifts to −33.5 mV after the second deposition cycles. However, when the $(TAPM/TPMC)_2$ membrane is deposited with another layer of TAPM, the zeta potential reverses to 29.0 mV. Furthermore, the absolute value of the zeta potential for the MLD membranes becomes less when the more cycles are adsorbed, which is in well agreement with other researchers.[40,41]

The water flux of our MLD membranes is much less than that of NF membranes with thicker skin layers via the interfacial polymerization technique. It can be explained in terms of the reduced porosity of the PAN-COOH support as well as the low roughness and hydrophilicity of the membrane surface. When the PAN-COOH was immersed in a solution of TAPM, TAPM would be retained to the pores due to the intrinsic capillarity of the porosity support. Thus, after the amine-terminated surface was sequentially submerged in a solution of TPMC, highly active acid chloride would react with primary amine in the pores as well, leading to narrowing the pores and then reducing the water flux. On the other hand, the water permeability of the entire membrane also correlates with morphology of the deposited polyamide layer. Figure 6 shows the representative AFM height images of five MLD multilayered films on PAN-COOH substrate. The root-mean-square (RMS) roughness, the mean of the root for the deviation from the standard surface to the indicated surface, decreases with increasing film thickness, and the value of $(TAPM/TPMC)_{30}$ is only 1.82 nm (Table 1), almost 2 orders of magnitude smaller than the thin film composite membranes prepared by interfacial polymerization.[21] The low RMS corresponds to a smooth surface of the membrane, indicating consistent growth over the substrate. On the other hand, contact angle (CA) is investigated to reflect the tendency for the water to wet the membrane surface. The lower

dx.doi.org/10.1021/la304196q | Langmuir 2012, 28, 17803−17810

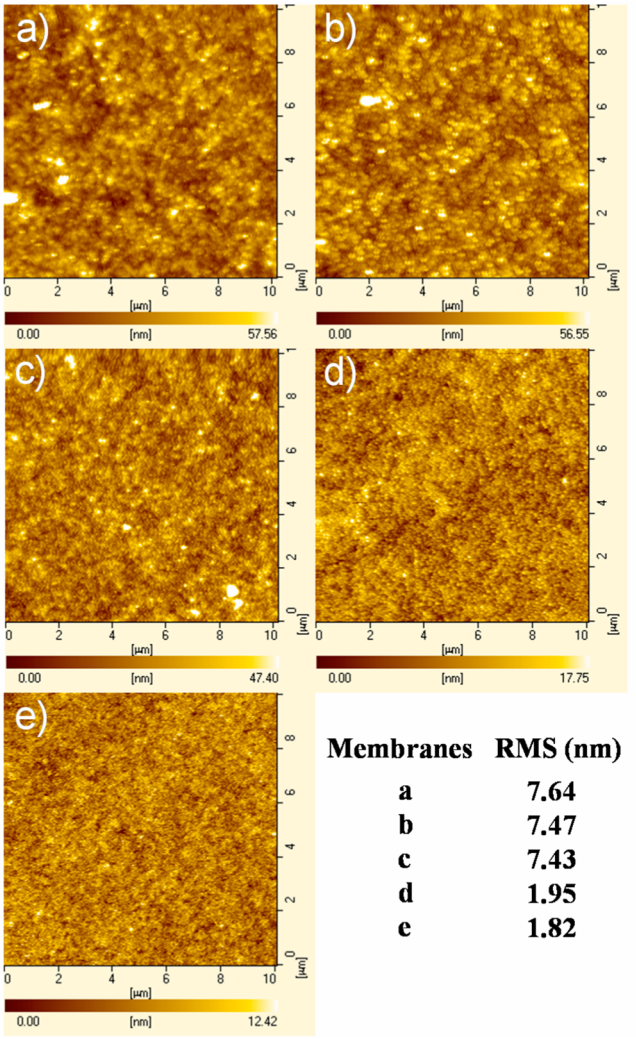

Membranes	RMS (nm)
a	7.64
b	7.47
c	7.43
d	1.95
e	1.82

Figure 6. AFM height images for MLD films on hydrolyzed PAN substrates with different deposition cycles: (a) 14.5, (b) 15, (c) 15.5, (d) 30, and (e) 30.5 cycles.

CA means a greater wettability and a higher hydrophilicity. It is expected that the hydrophilicity of the membrane surface will change with the addition of alternating TAPM and TPMC layers. Table 1 summarizes the CA of the MLD membranes on PAN-COOH substrate. The PAN-COOH substrate exhibits a CA of 28.4°, indicating the substrate is fairly hydrophilic. However, the surface becomes more and more hydrophobic when the number of deposition cycle increases. This result suggests the surface becomes more homogeneous and smoother, which was consistent with the results from AFM. The CA of successive deposition cycle membranes demonstrates the carboxylic acid-terminated surface is more hydrophilic than the amine moiety as the CA of 15-cycle membrane (65.6°) is lower than those of 14.5 (66.7°) and 15.5 cycles (69.1°).

The smooth surface of the resulting NF membranes is advantage in terms of fouling.[42] Thus, we test the long-term stability of $(TAPM/TPMC)_{30}$ membrane under operating pressure of 0.4 MPa with 500 mg/L Na_2SO_4 aqueous solution at 25.0 °C. The water flux and salt rejection of the studied membrane during the 20 days filtration are presented in Figure 7. The initial salt water flux is 10.2 L/(m^2 h), 9% less than the pure water flux of 11.2 L/(m^2 h) due to the increasing osmotic

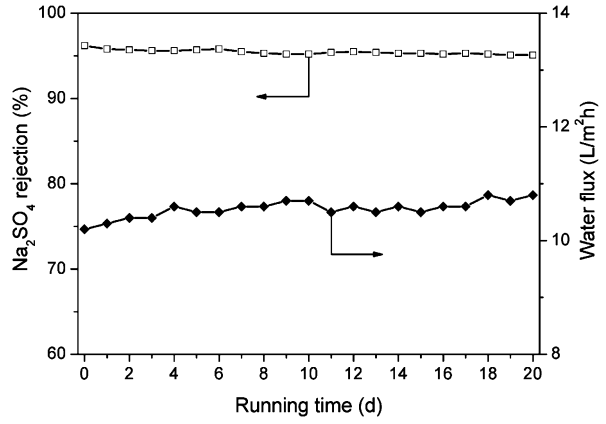

Figure 7. Variation of salt rejection and water flux as a function of running time for $(TAPM/TPMC)_{30}$ membrane tested with 500 mg/L Na_2SO_4 at 0.4 MPa and 25.0 °C.

pressure and concentration polarization near the membrane surface. In addition, the water flux of the membrane lies within the scope of 10.2−10.8 L/(m^2 h), while the overall Na_2SO_4 rejection keeps steady in the range of 95.1−96.2% during the whole testing period. The continuous test results indicate the MLD NF membrane possesses good durability and high long-term performance stability. The AFM image of $(TAPM/TPMC)_{30}$ membrane taken after performance testing for 20 days is shown in Figure S11. It can be seen that the morphology of tested membrane with RMS of 1.89 nm is nearly the same as that of the original membrane, verifying the stability of the MLD membranes.

CONCLUSIONS

In summary, we have demonstrated the controlled synthesis of ultrathin films of organic networks on various substrates via solution-based MLD that utilizes amide bond formation reaction between polyfunctional amine and acyl chloride with tetrahedral geometries. Characterization of films using UV−vis adsorption, ellipsometry, and quartz crystal microbalance indicate the linear and surface-limited growth behavior of the organic network, and the polyamide network was quite stable in a pH range of 1−10. The MLD growth rate is measured to be about 1.6 nm per cycle, in accordance with simulations based on the size of the molecules involved in the reaction. In the following, we develop the MLD method on the top of hydrolyzed PAN substrate, resulting in NF membranes. The separation performance of the obtained membrane for various solutes is sensitive to the terminated layers and number of cycles. The surface charge density of the membrane decreases with the addition of deposition layers. The moderate water flux for the resulting membrane is due to the reduced porosity of the PAN-COOH support as well as the low roughness and hydrophilicity of the membrane surface. The long-term filtration tests show the MLD membranes possess excellent durability and performance stability, indicating potentially attractive for water softening applications.

ASSOCIATED CONTENT

Supporting Information

Experimental procedures for syntheses of all the products; ^1H and ^{13}C NMR spectra of all the products; UV−vis spectra of 30-cycle multilayered pristine film and soaked at pH 10 and 1; the simulative molecular structures of TPMC and TAPM; FT-

dx.doi.org/10.1021/la304196q | Langmuir 2012, 28, 17803−17810

IR spectra of TAPM, TPMC, and BPA; ATR-IR spectra of initial PAN and hydrolyzed PAN substrates; intergrated absorbance of peaks at 2244 and 1542 cm^{-1} with increasing number of MLD cycles; AFM image of MLD membrane taken after long-term testing. This material is available free of charge via the Internet at http://pubs.acs.org.

AUTHOR INFORMATION

Corresponding Author

*Tel +86 (0) 431 85262118; Fax +86 (0) 431 85262117; e-mail sbzhang@ciac.jl.cn.

Notes

The authors declare no competing financial interest.

ACKNOWLEDGMENTS

We thank the National Basic Research Program of China (No. 2009CB623401 and 2012CB932802) and the National Science Foundation of China (No. 51133008, 50825302, and 51021003). H.Q. thanks Ms. Yuqi Liu in CIAC for her help in molecular simulations.

REFERENCES

(1) Thomas, A.; Kuhn, P.; Weber, J.; Titirici, M. M.; Antonietti, M. Porous polymers: enabling solutions for energy applications. *Macromol. Rapid Commun.* **2009**, *30*, 221−236.

(2) Lee, B. H.; Ryu, M. K.; Choi, S. Y.; Lee, K. H.; Im, S.; Sung, M. M. Rapid vapor-phase fabrication of organic-inorganic hybrid superlattices with monolayer precision. *J. Am. Chem. Soc.* **2007**, *129*, 16034−16041.

(3) Peyratout, C. S.; Dahne, L. Tailor-made polyelectrolyte microcapsules: From multilayers to smart containers. *Angew. Chem., Int. Ed.* **2004**, *43*, 3762−3783.

(4) Zelikin, A. N.; Li, Q.; Caruso, F. Degradable polyelectrolyte capsules filled with oligonucleotide sequences. *Angew. Chem., Int. Ed.* **2006**, *45*, 7743−7745.

(5) Such, G. K.; Johnston, A. P. R.; Caruso, F. Engineered hydrogen-bonded polymer multilayers: from assembly to biomedical applications. *Chem. Soc. Rev.* **2011**, *40*, 19−29.

(6) Such, G. K.; Quinn, J. F.; Quinn, A.; Tjipto, E.; Caruso, F. Assembly of ultrathin polymer multilayer films by click chemistry. *J. Am. Chem. Soc.* **2006**, *128*, 9318−9319.

(7) Quinn, J. F.; Johnston, A. P. R.; Such, G. K.; Zelikin, A. N.; Caruso, F. Next generation, sequentially assembled ultrathin films: beyond electrostatics. *Chem. Soc. Rev.* **2007**, *36*, 707−718.

(8) Buck, M. E.; Zhang, J.; Lynn, D. M. Layer-by-layer assembly of reactive ultrathin films mediated by click-type reactions of poly(2-alkenyl azlactone)s. *Adv. Mater.* **2007**, *19*, 3951−3955.

(9) Buck, M. E.; Schwartz, S. C.; Lynn, D. M. Superhydrophobic thin films fabricated by reactive layer-by-layer assembly of azlactone-functionalized polymers. *Chem. Mater.* **2010**, *22*, 6319−6327.

(10) Broderick, A. H.; Lynn, D. M. Covalent Layer-by-Layer Assembly Using Reactive Polymers. In *Functional Polymers by Post-Polymerization Modification: Concepts, Practical Guidelines, and Applications*; Theato, P., Klok, H. A., Eds.; Wiley-VCH: New York, 2012; pp 371−406.

(11) Yoshimura, T.; Tatsuura, S.; Sotoyama, W. Polymer-films formed with monolayer growth steps by molecular Layer deposition. *Appl. Phys. Lett.* **1991**, *59*, 482−484.

(12) Du, Y.; George, S. M. Molecular layer deposition of nylon 66 films examined using in situ FTIR spectroscopy. *J. Phys. Chem. C* **2007**, *111*, 8509−8517.

(13) Adarnczyk, N. M.; Dameron, A. A.; George, S. M. Molecular layer deposition of poly(p-phenylene terephthalamide) films using terephthaloyl chloride and p-phenylenediamine. *Langmuir* **2008**, *24*, 2081−2089.

(14) Putkonen, M.; Harjuoja, J.; Sajavaara, T.; Niinisto, L. Atomic layer deposition of polyimide thin films. *J. Mater. Chem.* **2007**, *17*, 664−669.

(15) Lee, J. S.; Lee, Y. J.; Tae, E. L.; Park, Y. S.; Yoon, K. B. Synthesis of zeolite as ordered multicrystal arrays. *Science* **2003**, *301*, 818−821.

(16) Kim, A.; Filler, M. A.; Kim, S.; Bent, S. F. Layer-by-layer growth on Ge(100) via spontaneous urea coupling reactions. *J. Am. Chem. Soc.* **2005**, *127*, 6123−6132.

(17) George, S. M.; Yoon, B.; Dameron, A. A. Surface chemistry for molecular layer deposition of organic and hybrid organic-inorganic polymers. *Acc. Chem. Res.* **2009**, *42*, 498−508.

(18) Loscutoff, P. W.; Zhou, H.; Clendenning, S. B.; Bent, S. F. Formation of organic nanoscale laminates and blends by molecular layer deposition. *ACS Nano* **2010**, *4*, 331−341.

(19) Kim, M.; Byeon, M.; Bae, J. S.; Moon, S. Y.; Yu, G.; Shin, K.; Basarir, F.; Yoon, T. H.; Park, J. W. Preparation of ultrathin films of molecular networks through layer-by-layer cross-linking polymerization of tetrafunctional monomers. *Macromolecules* **2011**, *44*, 7092−7095.

(20) Steiner, Z.; Miao, J.; Kasher, R. Development of an oligoamide coating as a surface mimetic for aromatic polyamide films used in reverse osmosis membranes. *Chem. Commun.* **2011**, *47*, 2384−2386.

(21) Johnson, P. M.; Yoon, J.; Kelly, J. Y.; Howarter, J. A.; Stafford, C. M. Molecular layer-by-layer deposition of highly crosslinked polyamide films. *J. Polym. Sci., Part B: Polym. Phys.* **2012**, *50*, 168−173.

(22) Lu, W. G.; Yuan, D. Q.; Zhao, D.; Schilling, C. I.; Plietzsch, O.; Muller, T.; Brase, S.; Guenther, J.; Blumel, J.; Krishna, R.; Li, Z.; Zhou, H. C. Porous polymer networks: synthesis, porosity, and applications in gas storage/separation. *Chem. Mater.* **2010**, *22*, 5964−5972.

(23) Oh, N. W.; Jegal, J.; Lee, K. H. Preparation and characterization of nanofiltration composite membranes using polyacrylonitrile (PAN). I. Preparation and modification of PAN supports. *J. Appl. Polym. Sci.* **2001**, *80*, 1854−1862.

(24) Weber, J.; Antonietti, M.; Thomas, A. Microporous networks of high-performance polymers: Elastic deformations and gas sorption properties. *Macromolecules* **2008**, *41*, 2880−2885.

(25) Peng, B.; Wu, G. J.; Lin, Y.; Wang, Q.; Su, Z. H. Preparation of nanoporous polyimide thin films via layer-by-layer self-assembly of cowpea mosaic virus and poly(amic acid). *Thin Solid Films* **2011**, *519*, 7712−7716.

(26) Liu, M. H.; Wu, D. H.; Yu, S. C.; Gao, C. J. Influence of the polyacyl chloride structure on the reverse osmosis performance, surface properties and chlorine stability of the thin-film composite polyamide membranes. *J. Membr. Sci.* **2009**, *326*, 205−214.

(27) Childress, A. E.; Elimelech, M. Effect of solution chemistry on the surface charge of polymeric reverse osmosis and nanofiltration membranes. *J. Membr. Sci.* **1996**, *119*, 253−268.

(28) Nadler, R.; Srebnik, S. Molecular simulation of polyamide synthesis by interfacial polymerization. *J. Membr. Sci.* **2008**, *315*, 100−105.

(29) Seo, J.; Schattling, P.; Lang, T.; Jochum, F.; Nilles, K.; Theato, P.; Char, K. Covalently bonded layer-by-layer assembly of multifunctional thin films based on activated esters. *Langmuir* **2010**, *26*, 1830−1836.

(30) Lee, C. T.; Yang, W. T.; Parr, R. G. Development of the Colle-Salvetti correlation-energy formula into a functional of the electron-density. *Phys. Rev. B* **1988**, *37*, 785−789.

(31) Becke, A. D. Density-functional thermochemistry. 3. The role of exact exchange. *J. Chem. Phys.* **1993**, *98*, 5648−5652.

(32) Frisch, M. J.; Trucks, G. W.; Schlegel, H. B.; Scuseria, G. E.; Robb, M. A.; Cheeseman, J. R.; Scalmani, G.; Barone, V.; Mennucci, B.; Petersson, G. A.; et al. *GAUSSIAN 09 (Revision B.01)*; Gaussian, Inc.: Wallingford, CT, 2010.

(33) Chiang, Y. C.; Hsub, Y. Z.; Ruaan, R. C.; Chuang, C. J.; Tung, K. L. Nanofiltration membranes synthesized from hyperbranched polyethyleneimine. *J. Membr. Sci.* **2009**, *326*, 19−26.

(34) Malaisamy, R.; Bruening, M. L. High-flux nanofiltration membranes prepared by adsorption of multilayer polyelectrolyte membranes on polymeric supports. *Langmuir* **2005**, *21*, 10587−10592.

(35) Qiu, C. Q.; Qi, S. R.; Tang, C. Y. Y. Synthesis of high flux forward osmosis membranes by chemically crosslinked layer-by-layer polyelectrolytes. *J. Membr. Sci.* **2011**, *381*, 74−80.
(36) Stanton, B. W.; Harris, J. J.; Miller, M. D.; Bruening, M. L. Ultrathin, multilayered polyelectrolyte films as nanofiltration membranes. *Langmuir* **2003**, *19*, 7038−7042.
(37) Wang, H. F.; Zhang, Q. F.; Zhang, S. B. Positively charged nanofiltration membrane formed by interfacial polymerization of 3,3′,5,5′-biphenyl tetraacyl chloride and piperazine on a poly(acrylonitrile) (PAN) support. *J. Membr. Sci.* **2011**, *378*, 243−249.
(38) Bason, S.; Freger, V. Phenomenological analysis of transport of mono- and divalent ions in nanofiltration. *J. Membr. Sci.* **2010**, *360*, 389−396.
(39) Egueh, A. N. D.; Lakard, B.; Fievet, P.; Lakard, S.; Buron, C. Charge properties of membranes modified by multilayer polyelectrolyte adsorption. *J. Colloid Interface Sci.* **2010**, *344*, 221−227.
(40) Adusumilli, M.; Bruening, M. L. Variation of ion-exchange capacity, zeta potential, and ion-transport selectivities with the number of layers in a multilayer polyelectrolyte film. *Langmuir* **2009**, *25*, 7478−7485.
(41) Ali, M.; Yameen, B.; Cervera, J.; Ramirez, P.; Neumann, R.; Ensinger, W.; Knoll, W.; Azzaroni, O. Layer-by-layer assembly of polyelectrolytes into ionic current rectifying solid-state nanopores: insights from theory and experiment. *J. Am. Chem. Soc.* **2010**, *132*, 8338−8348.
(42) Yu, S. C.; Ma, M.; Liu, J. Q.; Tao, J.; Liu, M. H.; Gao, C. J. Study on polyamide thin-film composite nanofiltration membrane by interfacial polymerization of polyvinylamine (PVAm) and isophthaloyl chloride (IPC). *J. Membr. Sci.* **2011**, *379*, 164−173.